



Title	An analysis of transverse evolution of electron swarms in gases using moment equations and a propagator method
Author(s)	Sugawara, Hirotake; Sakai, Yosuke
Citation	Journal of Physics D: Applied Physics, 32(14), 1671-1680 https://doi.org/10.1088/0022-3727/32/14/320
Issue Date	1999-07-21
Doc URL	http://hdl.handle.net/2115/13467
Rights	Copyright © 1999 Institute of Physics
Type	article (author version)
File Information	sugawara-jpd-1999.pdf



[Instructions for use](#)

An analysis of transverse evolution of electron swarms in gases using moment equations and a propagator method **z**

Hirotake Sugawara and Y Sakai

Division of Electronics and Information Engineering, Hokkaido University, Sapporo
060-8628 Japan

Abstract. A simulation technique for analysis of transverse evolution of electron swarms in gases was developed based on moment equations derived from the Boltzmann equation. A numerical calculation of the moment equations for an electron swarm was performed using a propagator method and it was demonstrated that the propagator method can be used to calculate the higher-order transverse diffusion coefficients stably. Applying a Hermite expansion technique, the electron distribution in real space and other electron swarm parameters were derived as functions of the transverse position. The calculation result was verified by comparisons with those by a Monte Carlo simulation and other methods. Features of the transverse electron swarm evolution were presented.

PACS numbers: 52.80.-s Electric discharges

1. Introduction

The evolution of electron swarms in gases has been studied as a fundamental approach to the engineering of weakly ionized plasmas. Typically, the primary purposes of investigations on electron swarms are analyses of essential features of electron swarm behavior and the derivation of quantitative data concerning the electron transport coefficients such as the drift velocity W and the diffusion coefficient D . These transport coefficients are, for example, referred to in fluid model simulations of processing plasmas, plasma display panels, gas lasers, light sources, etc, as key quantities that govern the characteristics of the plasmas.

Among various electron transport coefficients, the transverse diffusion coefficient D_{\perp} is focused on in the present paper. D_{\perp} is known as the time derivative of the second-

z Published source: Journal of Physics D: Applied Physics, Vol. 32 (1999), pp. 1671-1680.

order transverse spatial moment defined along the perpendicular direction relative to the applied electric field E . Here, it is noted that D_T is distinguished from the longitudinal diffusion coefficient D_L which is defined along the direction of E . D_T is an important quantity for discussing the diffusive loss of electrons to side walls of plasma reactors and discharge tubes. Knowledge of D_T may hopefully contribute to a realization of uniform large-area plasmas for mass processing and their control. One may need D_T and D_L values separately for advanced two-dimensional fluid model simulations in future in order to consider direction-dependent diffusion. Since no external transverse force works upon the electrons, the transverse diffusion of an electron swarm appears more spontaneous than the longitudinal diffusion along E .

In general, the diffusion of an electron swarm is not isotropic, i.e. $D_T \neq D_L$. Many references quoted in the present paper show $D_T > D_L$ except under particular conditions such as strong anisotropic scattering and low electric field as found in Kr and Xe (Dutton 1975), Ar (Braglia and Baiocchi 1978, Makabe and Shimoyama 1986) and CH_4 (Segur et al 1984). It is noted that these gases have the Ramsauer-Townsend minimum in their momentum transfer cross sections. The anisotropy and its transient behavior in short-time electron swarm evolution were analyzed by Skullerud (1974), Braglia (1977), Braglia and Baiocchi (1978), Kumar (1981) and McMahon et al (1986).

D_T values in real gases have been experimentally measured by a number of investigators. Early examples of the D_T measurements can be found in Naidu and Prasad (1972) for SF_6 , Blevin et al (1978) for H_2 , Fletcher and Reid (1980) for N_2 , etc.

On the other hand, mathematical descriptions relating D_T with other transport parameters were given by Tagashira et al (1977, 1978), Kitamori et al (1980), Kumar et al (1980), Ikuta and Nakajima (1993) and Robson (1995). Values of D_T in real gases were calculated using Boltzmann equation analyses, Monte Carlo simulations, and other numerical methods by Lowke et al (1973) for a $\text{CO}_2/\text{N}_2/\text{He}$ mixture, Pitchford and Phelps (1982) and Phelps and Pitchford (1985) for N_2 , Makabe and Shimoyama (1986) and Koura (1987) for Ar or an Ar-like gas, Yachi et al (1991) and Date et al (1993) for CH_4 , etc. D_T was also calculated for Ba^+ ions in Ar by Viehland (1994).

These experimental data and theoretical calculation results of D_T were often compared in efforts to estimate the electron collision cross sections using data obtained by the swarm method: for example Itoh et al (1988, 1993) for SF_6 , Bordage et al (1996) for CF_4 and Yousfi and Benabdessadok (1996) for NH_3 .

D_T was also calculated in model gases for theoretical studies on anisotropic scattering, benchmark calculations of newly developed simulation techniques, etc: for example Pitchford et al (1981), Skullerud and Kuhn (1983), Skullerud (1984), Makabe and Mori (1984), Segur et al (1984), Penetrante et al (1985), Koura (1986), Ikuta and Murakami (1987) and Ikuta et al (1988).

In most of these references transverse properties of electron swarms are described

mainly by the second-order coefficient D_T . Only a few of them mention the higher-order coefficients $D_{T;n}$ ($n = 4; 6; 8; \dots$), and fewer still showed their quantitative results (e.g. Kitamori et al 1980).

In the present paper, a calculation technique applicable to derivation of higher-order parameters of the transverse electron swarm evolution is developed based on moment equations derived from the Boltzmann equation. Then a stable numerical calculation for the transverse moments and $D_{T;n}$ is demonstrated using a propagator method modified for the transverse calculation. A comparison between the transverse and longitudinal calculation schemes of the propagator method is presented and features of the transverse electron swarm evolution are investigated through an analysis of the position-dependent diffusive velocity and ionization.

2. Calculation method

2.1. Analysis model

The evolution of an electron swarm is considered in boundary-free real space $(r) = (x; y; z)$. A uniform electric field \mathbf{E} is applied in the x direction, and the initial electrons are supplied from a point source at the origin with an axially symmetric velocity distribution around the x axis.

The electron distribution function $f(r; v; t)$ at time t is defined in phase space $(r; v) = (x; y; z; v_x; v_y; v_z)$, and its temporal variation is described by the Boltzmann equation

$$\frac{\partial}{\partial t} f(r; v; t) = \mathbf{a} \cdot \nabla_v f(r; v; t) + \frac{\partial}{\partial t} \Big|_{\text{coll}} f(r; v; t) \quad (1)$$

where $\mathbf{a} = (a_x; 0; 0) = (eE_x/m; 0; 0)$ is the acceleration due to $\mathbf{E} = (E_x; 0; 0)$, e and m are the electron charge and mass and $(\partial/\partial t)_{\text{coll}}$ is the collision operator.

Instead of Cartesian coordinates $(v_x; v_y; v_z)$ for v , polar coordinates $(v; \hat{i}; \hat{c})$, the scalar electron speed and the polar and azimuthal angles, may be adopted relevantly in the descriptions. The relation between the two coordinate systems is defined as $(v_x; v_y; v_z) = (v \cos \hat{i}; v \sin \hat{i} \cos \hat{c}; v \sin \hat{i} \sin \hat{c})$ (see figure 1).

2.2. Moment equations

We calculate the n th-order spatial moment of an electron swarm with respect to the y direction. Its distribution $m_{y;n}(v; t)$ in velocity space and total amount $M_{y;n}(t)$ are defined as

$$m_{y;n}(v; t) = \int_{zr}^z y^n f(r; v; t) dr \quad (2)$$

$$M_{y;n}(t) = \int_v m_{y;n}(v; t) dv \quad (3)$$

It is noted that $m_{y,0}(v; t)$ and $M_{y,0}(t)$ are identical to the electron velocity distribution and the number of electrons, respectively.

A series of moment equations, which describe the temporal variation of $m_{y;n}(v; t)$, are derived by integrating equation (1) with the weight of y^n throughout (r)

$$\frac{\partial}{\partial t} m_{y;n} = \ddot{A} a_x \frac{\partial}{\partial v_x} m_{y;n} + n v_y m_{y;n} \ddot{A} + \frac{\partial}{\partial t} m_{y;n}^{\text{coll}} \quad (4)$$

The terms on the right-hand side of equation (4) correspond to acceleration, diffusion and collision processes, respectively.

In the previous work (Sugawara et al 1998), two coordinates v and \hat{r} were necessary to calculate the longitudinal moment distribution $m_{x;n}(v; t)$. Here one may simply integrate $m_{x;n}(v; t)$ with respect to \hat{u} because electrons with common velocity components $(v; \hat{r})$ are all equivalent in the contribution to the longitudinal moment equations irrespective of \hat{u} . On the other hand, in the case of $m_{y;n}(v; t)$, a difference in \hat{u} induces different contributions in the transverse moment equations through the diffusion term in equation (4) since a factor $\cos \hat{u}$ is included there as $v_y = v \sin \hat{r} \cos \hat{u}$.

However, in spite of the dependence of $m_{y;n}(v; t)$ on \hat{u} , an expansion for the azimuthal moment distribution enables us to reduce the velocity space down to two-dimensional $(v; \hat{r})$ similarly to the longitudinal case. By introducing the powers of $\cos \hat{u}$ as the bases of expansion, $m_{y;n}(v; t)$ can be expanded as

$$m_{y;n}(v; \hat{r}; \hat{u}; t) = \sum_{k=0}^{\infty} w_{n,k}(v; \hat{r}; t) \cos^k \hat{u} \quad (5)$$

where $w_{n,k}(v; \hat{r}; t)$ is the weight of the k th azimuthal component of the n th-order transverse moment. The transverse moment distributions in velocity space are localized around $\hat{u} = 0$ and $\hat{u} = \pi$ except for the zeroth-order one (see figure 2). A detailed derivation of this expansion is presented in Appendix A.

Applying equation (5) to equation (4), we obtain the evolution equations of $w_{n,k}(v; \hat{r}; t)$ to be calculated numerically by the present propagator method (see

subsection 2.4):

$$\begin{aligned}
(\partial_t)w_{0;0} &= \ddot{A}_x(\partial_{v_x})w_{0;0} + (\partial_t)_{\text{coll}}w_{0;0} \\
(\partial_t)w_{1;1} &= \ddot{A}_x(\partial_{v_x})w_{1;1} + v \sin \theta w_{0;0} + (\partial_t)_{\text{coll}}w_{1;1} \\
(\partial_t)w_{2;0} &= \ddot{A}_x(\partial_{v_x})w_{2;0} + (\partial_t)_{\text{coll}}w_{2;0} \\
(\partial_t)w_{2;2} &= \ddot{A}_x(\partial_{v_x})w_{2;2} + 2v \sin \theta w_{1;1} + (\partial_t)_{\text{coll}}w_{2;2} \\
(\partial_t)w_{3;1} &= \ddot{A}_x(\partial_{v_x})w_{3;1} + 3v \sin \theta w_{2;0} + (\partial_t)_{\text{coll}}w_{3;1} \\
(\partial_t)w_{3;3} &= \ddot{A}_x(\partial_{v_x})w_{3;3} + 3v \sin \theta w_{2;2} + (\partial_t)_{\text{coll}}w_{3;3} \\
(\partial_t)w_{4;0} &= \ddot{A}_x(\partial_{v_x})w_{4;0} + (\partial_t)_{\text{coll}}w_{4;0} \\
(\partial_t)w_{4;2} &= \ddot{A}_x(\partial_{v_x})w_{4;2} + 4v \sin \theta w_{3;1} + (\partial_t)_{\text{coll}}w_{4;2} \\
(\partial_t)w_{4;4} &= \ddot{A}_x(\partial_{v_x})w_{4;4} + 4v \sin \theta w_{3;3} + (\partial_t)_{\text{coll}}w_{4;4} \\
&\vdots
\end{aligned} \tag{6}$$

In the above equations, $w_{n;k}$ for $n \neq k \pmod{2}$ are missing since they are always zero as mentioned in Appendix A.

A component $w_{n;k}(v; \theta; t)$ affects others through the acceleration, diffusion and collision terms. A schematic for the action is shown in Figure 3.

2.3. Higher-order transverse diffusion coefficients

The electron transport coefficients have been systematized in attempts to expand the temporal variation of the electron distribution function using an infinite series of the electron number density gradient terms: for example Skullerud (1974), Tagashira et al (1977, 1978), Kitamori et al (1980), Kumar et al (1980), Kumar (1981), Standish (1987) and Kondo and Tagashira (1990). The transport coefficients are defined as the coefficients of the gradient terms and they have constant non-zero values in the hydrodynamic regime. Although there is no convenient experimental way to measure the higher-order coefficients directly, as mentioned by Kumar (1981), they can be derived from the spatio-temporal profile of the electron distribution as the time derivatives of certain spatial moments.

In fluid model simulations, the gradient expansion is often approximated by the second-order continuity equation truncating the higher-order terms. When the transport coefficients in the continuity equation, the ionization frequency R_i , the drift velocity W and the diffusion coefficient D , are constants independent of the position r as they are in the hydrodynamic regime, the continuity equation is identical to the diffusion equation. A Gaussian distribution for the spatial electron distribution $p(r; t)$ is an analytical solution of the diffusion equation and it represents the primary characteristics of the electron swarm evolution well. However, practical $p(r; t)$ may have a skewed shape deviated from a Gaussian distribution especially in the initial relaxation processes.

The entire gradient expansion including the higher-order terms could cover even such a distorted shape, thus the higher-order transport coefficients are understood as modification factors for the Gaussian solution (Skullerud 1974, Tagashira et al 1977).

With respect to the transverse evolution of an electron swarm, the n th-order transverse diffusion coefficients $D_{T;n}$ ($n = 2; 4; 6; \dots$, $D_{T;2} = D_T$) are defined as the coefficients of the density gradient terms in a continuity equation in the y direction:

$$\frac{\partial}{\partial t} p(y; t) = \frac{\partial}{\partial z} \left(R_i + D_T \frac{\partial}{\partial y^2} + D_{T;4} \frac{\partial^4}{\partial y^4} + D_{T;6} \frac{\partial^6}{\partial y^6} + \dots \right) p(y; t) \quad (7)$$

$$p(y; t) = \int_{-\infty}^{\infty} \int_{-\infty}^{\infty} f(r; v; t) dx dz dv \quad (8)$$

Being different from a longitudinal continuity equation, the terms of odd orders are missing in equation (7) because their coefficients are zero due to the symmetry of $p(y; t)$.

$D_{T;n}$ can be derived from the moments $M_{y;n}(t)$ in the same way as done for $D_{L;n}$ by Tagashira et al (1977) and Sugawara et al (1998):

$$D_{T;n}(t) = \frac{1}{n!} \frac{d}{dt} \frac{M_{y;n}(t)}{M_{y;0}(t)} \stackrel{n \geq 1}{=} \sum_{k=1}^{n-2} \frac{D_{T;2k}(t)}{(n-2k)!} \frac{M_{y;n-2k}(t)}{M_{y;0}(t)}. \quad (9)$$

To be exact, we should mention that the higher-order diffusion coefficient is essentially not the time derivative of the moment but the time derivative of a statistical quantity called the cumulant (Sugawara et al 1998). The cumulant is recognized as a quantity that represents the degree of the deviation of a distribution shape from a Gaussian distribution since the higher-order cumulants of a Gaussian distribution are all zero.

The normalized n th-order cumulants $\hat{\Gamma}_{x;n}$ and $\hat{\Gamma}_{y;n}$, respectively, defined for the longitudinal and transverse electron distribution functions, give the higher-order longitudinal and transverse diffusion coefficients as follows:

$$D_{L;n} = \frac{1}{n!} \frac{d}{dt} \hat{\Gamma}_{x;n} \quad (\text{for } n = 2; 3; 4; \dots) \quad (10)$$

$$D_{T;n} = \frac{1}{n!} \frac{d}{dt} \hat{\Gamma}_{y;n} \quad (\text{for } n = 2; 4; 6; \dots) \quad (11)$$

Since the definition of the cumulants using the cumulant-generating function derived from the moment-generating function is more or less abstract, it is not easy to understand their physical meaning intuitively.

2.4. Propagator method

Propagator method (PM) is a computational technique for $f(r; v; t)$. The phase space $(r; v)$ is divided into small sections called cells and $f(r; v; t)$ is represented using an array of the number of electrons in each cell. The temporal variation of $f(r; v; t)$ due

to drift and collision processes is treated as intercellular motion of electrons. Their destinations and transition rates are described using a transition probability function called a propagator or Green's function, which is determined based on Newton's motion equation and the collision probability quantified by the electron collision cross sections.

Sugawara et al (1998) applied a PM for a calculation of the longitudinal moment equations. This technique is modified for the present transverse analysis.

As mentioned in section 2.2, the dependence of $m_{y;n}(v; t)$ on \hat{u} can be treated separately from that on v and \hat{i} by introducing the azimuthal expansion. Two-dimensional velocity space $(v; \hat{i})$ is sufficient to operate $m_{y;n}(v; t)$ in terms of $w_{n;k}(v; \hat{i}; t)$. The azimuthal expansion induces the increase in the number of components or equations to be calculated simultaneously. While a longitudinal analysis up to the n th order requires $(n + 1)$ components, the transverse case in the same order requires roughly $(n + 2)^2 = 4$ components. Nonetheless, the advantage of the dimension reduction exceeds the increase of the components from the viewpoint of the computational load.

The velocity space $(v; \hat{i})$ is divided into cells $\Delta v \Delta \hat{i}$ in the same way as in the previous work. A cell is to have values of $w_{n;k}(v; \hat{i}; t) \Delta v \Delta \hat{i}$. These values originate from the electrons in the cell. In the present calculation, $m_{y;n}(v; t)$ is calculated up to $n = 6$, that requires 16 components of $w_{n;k}(v; \hat{i}; t)$ for the transverse calculation. An accompanying calculation of $m_{x;n}(v; t)$ up to the same order would require six more components ($m_{x;1}$ through $m_{x;6}$), where $m_{x;0}$ and $m_{y;0}$ are identical to each other. A customized implementation for the electron transport coefficients up to the second order would require six components in total.

3. Results and discussion

3.1. Benchmark calculation with model gases

For verification of the present technique, electron swarm parameters in ramp and step excitation model gases (Reid 1979) are calculated. These model gases have often been adopted for the verification of simulation methods: for example Pitchford et al (1981), Segur et al (1984), Penetrante et al (1985) and Yachi et al (1991). The model gases have the electron collision cross sections of momentum transfer ($q_{\text{ramp};m}$ and $q_{\text{step};m}$) and excitation ($q_{\text{ramp};ex}$ and $q_{\text{step};ex}$ with the threshold of 0.2 eV):

$$q_{\text{ramp};m} = q_{\text{step};m} = \begin{cases} 6.0 \times 10^{-16} \text{ cm}^2 & \text{for } \epsilon < 0.2 \text{ eV} \\ < 0 \text{ cm}^2 & \text{for } \epsilon \geq 0.2 \text{ eV} \end{cases} \quad (12)$$

$$q_{\text{ramp};ex} = \begin{cases} 10.0 \times 10^{-16} \text{ cm}^2 & \text{for } \epsilon < 0.2 \text{ eV} \\ < 0 \text{ cm}^2 & \text{for } \epsilon \geq 0.2 \text{ eV} \end{cases} \quad (13)$$

$$q_{\text{step};ex} = \begin{cases} 10.0 \times 10^{-16} \text{ cm}^2 & \text{for } \epsilon < 0.2 \text{ eV} \\ < 0 \text{ cm}^2 & \text{for } \epsilon \geq 0.2 \text{ eV} \end{cases} \quad (14)$$

The initial electrons are supplied from the origin with the Maxwellian velocity distribution with a mean electron energy of $\bar{\epsilon} = 0.1$ eV. The reduced electric field E/N is assumed to be 1, 12 and 24 Td ($1 \text{ Td} = 10^{17} \text{ V cm}^{-2}$), at which data for comparison are available. The molecular number density N is $3.5 \times 10^{16} \text{ cm}^{-3}$ at 273 K at 133 Pa.

Equilibrium values of $\bar{\epsilon}$, W , D_L and D_T of the ramp and step model gases calculated by the present PM are listed in tables 1 and 2 together with those obtained by different methods. The swarm parameters are in good agreement with discrepancies less than one per cent for D_T and a few per cent for D_L . It can be confirmed that the derivation of the transverse moment equations and their numerical calculation are appropriate.

Table 1. **Electron swarm parameters in Reid's ramp excitation model gas:** MC, Monte Carlo simulation (Reid 1979); FEM, finite element method (Segur et al 1984); PDM, path differential method (Segur et al 1984); and PM, propagator method.

E=N (Td)	method	$\bar{\epsilon}$ (eV)	W (10^6 cm s^{-1})	ND_L ($10^{22} \text{ cm}^{-1} \text{ s}^{-1}$)	ND_T ($10^{22} \text{ cm}^{-1} \text{ s}^{-1}$)
1	MC	0.1013	1.255		
	FEM	0.1015	1.271	0.7594	0.9749
	PDM	0.1018	1.270	0.7623	0.9735
	PM	0.1020	1.285	0.773	0.977
12	MC		6.87		
	FEM	0.2689	6.832	0.569	1.135
	PDM	0.269	6.832	0.569	1.131
	PM	0.2690	6.826	0.572	1.137
24	MC	0.408	8.883		
	FEM	0.4074	8.881	0.463	1.134
	PDM	0.4083	8.874	0.4613	1.131
	PM	0.4081	8.875	0.464	1.137

3.2. Evolution of the azimuthal components of the transverse moments

A calculation of the higher-order azimuthal components of the transverse moments are demonstrated taking SF_6 as an example of the real gases. SF_6 involves processes of elastic collision, electron attachment, vibrational and electronic state excitations and ionization. The electron transport properties of SF_6 were surveyed by Morrow (1986). The set of the electron collision cross sections of SF_6 is taken from Itoh et al (1988, 1993), in which the cross section set was improved so that experimental data of D_T can be reproduced in addition to the effective ionization coefficient, the drift velocity and D_L .

Table 2. **Electron swarm parameters in Reid's step excitation model gas: FEM, finite element method (Segur et al 1984); PDM, path differential method (Segur et al 1984); and PM, propagator method.**

E=N (Td)	method	$\bar{\epsilon}$ (eV)	W (10^6 cm s^{-1})	ND_L ($10^{22} \text{ cm}^{-1} \text{ s}^{-1}$)	ND_T ($10^{22} \text{ cm}^{-1} \text{ s}^{-1}$)
1	FEM	0.0761	1.506	0.7447	0.819
	PDM	0.0755	1.515	0.7487	0.811
	PM	0.0767	1.522	0.7619	0.821
12	FEM	0.1211	8.253	0.2948	0.4691
	PDM	0.1202	8.231	0.2954	0.4537
	PM	0.1216	8.276	0.3019	0.4710
24	FEM	0.192	10.53	0.234	0.4285
	PDM	0.192	10.63	0.236	0.4236
	PM	0.1933	10.54	0.2425	0.4290

Figure 4 shows experimental data of ND_L by Aschwanden (1985) and ND_T by Naidu and Prasad (1972) (references in Itoh et al 1993) and their extrapolated values using the cross sections from Itoh et al (1988, 1993). In the following calculation for the relaxation process of an electron swarm, $E=N$ is set at a high value of 1414 Td so that the electron swarm could reach equilibrium in a short time. The initial electrons are released from the origin with the Maxwellian velocity distribution with $\bar{\epsilon}=1.0$ eV.

Figure 5 shows the evolution of $w_{n;k}$ and their sum $M_{y;n}$ calculated by the present PM together with $M_{y;n}$ by a Monte Carlo simulation (MC). Here, $w_{n;k}$ are shown as the integrated amounts of $w_{n;k}(v; t)$ throughout (v) . The results of $M_{y;n}$ obtained by the two methods agree well with each other. However, resolution of $M_{y;n}$ into $w_{n;k}$ by the MC was difficult to do due to statistical fluctuation even with the number of electrons exceeding 10^6 , which may be related to the fact that the series of azimuthal expansion bases $\mathbf{f} \cos^k \theta$ is not an orthogonal system of functions.

After relaxation, each of the $w_{n;k}$ seems to have a particular dependence on t as $w_{n;k} \propto t^{(n-k)/2}$. Thus, we obtain $M_{y;n} \propto t^{n/2}$ because the isotropic component $w_{n;0}$ with the highest order of the dependence on t becomes the most dominant among the azimuthal components of $M_{y;n}$. That implies that the transverse moment distribution in velocity space tends to become isotropic with time.

Although the dependence of higher-order $M_{y;n}$ ($n \geq 4$) on t is not linear, the values of $D_{T;n}$ defined by equation (9) should become constants in the hydrodynamic regime. It should be noted that the right-hand side of equation (9) guarantees that all of the non-linear contribution of different orders of $M_{y;n}$ are always cancelled out.

Figure 6 shows the relaxation processes of various diffusion coefficients. $D_{v,k}$ and

$D_{v\parallel}$ are ones derived from the electron velocity components parallel and perpendicular to E . It is demonstrated that the PM can derive higher-order diffusion coefficients in a stable manner.

3.3. The transverse electron distribution in real space

Based on a series of the spatial moments of an electron swarm calculated in velocity space, we can compose the transverse electron distribution $p(y; t)$ in real space using a Hermite expansion technique (Sugawara et al 1998). $p(y; t)$ can be obtained as

$$p(y; t) = \frac{1}{\sqrt{2\tilde{\sigma}_y(t)}} \sum_{n=0}^{\infty} C_{y;n}(t) H_n \left(\frac{y}{\sqrt{2\tilde{\sigma}_y(t)}} \right) \exp \left(-\frac{y^2}{2[\tilde{\sigma}_y(t)]^2} \right) \quad (15)$$

where H_n is the n th-order Hermite polynomial, $C_{y;n}$ is the weight of the n th-order Hermite component $H_n(Y) \exp(-Y^2)$, $\tilde{\sigma}_y$ is the standard deviation of $p(y; t)$, and $\frac{y}{\sqrt{2\tilde{\sigma}_y}}$ is the unit length introduced to reduce the position y to be dimensionless as $Y = \frac{y}{\sqrt{2\tilde{\sigma}_y}}$. $p(y; t)$ consists of the Hermite components of even orders since $p(y; t)$ is symmetric in $y = 0$. In the present analysis, $C_{y;n}$ can be obtained up to $n = 6$ as follows:

$$\begin{aligned} 0! \tilde{\sigma}_y C_{y;0} &= M_{y;0} \\ 2! \tilde{\sigma}_y^3 C_{y;2} &= M_{y;2} - \tilde{\sigma}_y^2 M_{y;0} = 0 \\ 4! \tilde{\sigma}_y^5 C_{y;4} &= M_{y;4} - 6\tilde{\sigma}_y^4 M_{y;2} + 3M_{y;0} \\ 6! \tilde{\sigma}_y^7 C_{y;6} &= M_{y;6} - 15\tilde{\sigma}_y^6 M_{y;4} + 45\tilde{\sigma}_y^4 M_{y;2} - 15M_{y;0} \end{aligned} \quad (16)$$

Figure 7 shows $p(y; t)$ calculated by the MC and PM in SF₆ at $E/N = 1414$ Td. It is observed that the electron swarm evolves by diffusion and electron multiplication due to ionization.

For a normalized distribution with a Gaussian shape, $C_{y;0} = 1/\sqrt{2\tilde{\sigma}_y}$ and $C_{y;n} = 0$ for $n \neq 0$, thus $C_{y;n}$ can be used to quantify how close $p(y; t)$ is to a Gaussian distribution as well as the cumulants, i.e. $C_{y;4}$, $C_{y;6}$, $C_{y;8}$, etc. represent the distortion of $p(y; t)$. It is noted here that the absolute amounts of the cumulants, which may have physical dimension, increase linearly when $D_{L;n}$ and $D_{T;n}$ are constants, that is concluded from equations (10) and (11). On the other hand, higher-order $C_{x;n}$ and $C_{y;n}$, which are dimensionless quantities, decrease with time as shown after this. An advantage of the evaluation of distribution shapes with $C_{x;n}$ and $C_{y;n}$ is that the Hermite components have visual shapes; in contrast to this the definition of the cumulants is abstract.

Sugawara et al (1998) demonstrated the convergence of $p(x; t)$ to a Gaussian distribution by means of $C_{x;n}$ in the previous longitudinal analysis. Similar results for $p(y; t)$ can be seen in Figure 8. $C_{y;4}$ and $C_{y;6}$ calculated in the ramp model gas at $E/N = 24$ Td and in SF₆ at 1414 Td are to a sufficient extent smaller than the primary

component $C_{y,0}$. They tend to zero with time, that convinces us anew that $p(y; t)$ also converges to a Gaussian distribution.

3.4. The diffusive velocity and the standard deviation

As well as $p(y; t)$, the electron velocity distribution in real space can also be derived by the velocity-weighted Hermite expansion. Figure 9 shows $\bar{v}_y(y; t)$ defined as the mean value of v_y at position y , which is called the transverse diffusive velocity hereafter. The definition of \bar{v}_y is given as

$$\bar{v}_y(y; t) = \frac{\int_{-\infty}^{\infty} \int_{-\infty}^{\infty} v_y f(r; v; t) dx dz dv}{\int_{-\infty}^{\infty} f(r; v; t) dx dz dv} \quad (17)$$

\bar{v}_y proves to be linearly dependent on y as is concluded analytically under an assumption that the transverse electron swarm evolution can be described by the second-order diffusion equation (see Appendix B).

Figure 10 shows the temporal variation of $\bar{v}_y(y; t)$. The values of \bar{v}_y at $y = \bar{y}_0$ move on a pair of hyperbolic curves with time as indicated by the full circles. The deviation of $\bar{v}_y(\bar{y}_0)$ at $t = 4$ ns from the curves implies that D_T is still under relaxation at the moment as shown subsequently in Figure 11 (a).

When the number of electrons is conservative, an interesting result is

$$\bar{v}_y(\bar{y}_0)\bar{y}_0 = D_T \quad (18)$$

A numerical example supporting this result is presented in Figure 11 (a). The above relation seems to be satisfied not only in equilibrium but also during the relaxation period in the present conservative case.

On the other hand, Figure 11 (b) shows that $\bar{v}_y(\bar{y}_0)\bar{y}_0 < D_T$ in SF_6 in which frequent ionization is present, although the effect of ionization is taken into account in the derivation of equation (18) in Appendix B. This disagreement in the non-conservative case can be understood considering the following expression for D_T :

$$D_T = \int_{-\infty}^{\infty} \bar{v}_y(y; t) y p(y; t) dy + \frac{1}{2} \int_{-\infty}^{\infty} [R_i(y; t) - \bar{R}_i(t)] y^2 p(y; t) dy \quad (19)$$

where $R_i(y; t)$ and $\bar{R}_i(t)$ are the local and global averages of the effective ionization frequency of the electron swarm. The first and second terms on the right-hand side of equation (19) correspond to the diffusion and collision terms, respectively. When the second term is missing, we obtain equation (18) from equation (19). Thus the difference between $\bar{v}_y(\bar{y}_0)\bar{y}_0$ and D_T is attributed to non-uniformity of $R_i(y; t)$. A possible explanation for this view is given as follows. Ionization tends to occur in the leading part of an electron swarm where electrons have diffused more widely than in the other part of the swarm. The second-order moment is generated particularly in a region where y^2 is large. This view would be supported by the dependence of R_i on y shown in Figure 12.

The mechanism to determine whether $\bar{v}_y(\bar{\sigma}_y)\bar{\sigma}_y > D_T$ or $\bar{v}_y(\bar{\sigma}_y)\bar{\sigma}_y < D_T$ seems similar to that discussed by Sugawara et al (1997) for the center-of-mass drift velocity W_r and the average electron velocity W_v : whether $W_r > W_v$ or $W_r < W_v$. More detailed investigation for this relation would be attempted in succeeding work with the present analysis technique.

4. Conclusions

A numerical calculation technique for analysis of transverse evolution of electron swarms in gases was developed based on moment equations. Introducing an azimuthal expansion for the moment distribution function in velocity space, the higher-order transverse moments and diffusion coefficients were calculated up to the sixth order using a propagator method. It was demonstrated that the propagator method is numerically stable in calculations of the higher-order diffusion coefficients $D_{T;n}$. The validity of the present calculation method was verified in a benchmark calculation with model gases and a comparison with the result of a Monte Carlo simulation.

The properties of transverse electron diffusion in real space were analyzed using a Hermite expansion technique. It was quantitatively confirmed that the transverse electron distribution after relaxation can be approximated as a Gaussian distribution with little discrepancy.

The transverse diffusive velocity \bar{v}_y was defined as being the mean velocity in the transverse direction y . A calculation result and an analytical derivation showed that the local value of \bar{v}_y at position y , $\bar{v}_y(y)$, has linear dependence on y . Based on this fact, a relation $\bar{v}_y(\bar{\sigma}_y)\bar{\sigma}_y = D_{T;n}$ was derived for electron swarms subject to the second-order diffusion equation, where $\bar{\sigma}_y$ is the standard deviation. This relation was satisfied when the number of electrons is conservative; this was confirmed numerically as well. In the presence of ionization and/or electron attachment, the relation was not satisfied due to the non-uniformity of the spatial distribution of the transverse moment generation. It was shown that the local values of the mean electron energy and the effective ionization frequency increase with the transverse distance from the center of the electron swarm diffusion.

Acknowledgments

The authors wish to thank Professor Hiroyuki Date of Hokkaido University, Professor Hiroaki Tagashira and Professor Kohki Satoh of Muroran Institute of Technology for valuable discussions.

Appendix A. Azimuthal expansion of the transverse moment distribution

The azimuthal expansion of the transverse moment distribution $m_{y;n}(v; t)$ in equation (5) is explained in the manner of mathematical induction.

Let us assume the following expansion with the bases of $\mathbf{f} \cos^k \hat{\mathbf{U}}_y$ and their weights $w_{n;k}(v; \hat{\mathbf{r}}; t)$:

$$m_{y;n}(v; \hat{\mathbf{r}}; \hat{\mathbf{U}}; t) = \sum_{k=0}^n w_{n;k}(v; \hat{\mathbf{r}}; t) \cos^k \hat{\mathbf{U}}_y \quad (\text{A1})$$

For $n = 0$, $m_{y;0}(v; t)$ is identical to the electron velocity distribution. Since the initial electrons are given at the origin with an axially symmetric velocity distribution, we obtain $m_{y;0}(v; \hat{\mathbf{r}}; \hat{\mathbf{U}}; 0) = w_{0;0}(v; \hat{\mathbf{r}}; 0)$ and $m_{y;n}(v; \hat{\mathbf{r}}; \hat{\mathbf{U}}; 0) = 0$ ($n \geq 1$), that satisfy equation (A1).

The temporal variation of $m_{y;n}$ and their hierarchy is described by equation (4), which can be considered as a recurrence formula to derive the expansion bases of higher order $m_{y;n}$:

$$\frac{\partial}{\partial t} m_{y;n} = \mathbf{A} \cdot \mathbf{a}_x \frac{\partial}{\partial v_x} m_{y;n} + n v_y m_{y;n-1} + \frac{\partial}{\partial t}_{\text{coll}} m_{y;n} \quad (\text{A2})$$

$m_{y;n}(v; t)$ on the left-hand side of the equation (A2) inherits the expansion bases included in or generated by the terms in the right-hand side.

The acceleration term which induces a parallel shift of electrons in velocity space does not introduce any new expansion bases to $m_{y;n}$. It may change only the weights of the azimuthal components conventionally included in $m_{y;n}$.

The diffusion term raises the orders of bases of $m_{y;n-1}$ when $m_{y;n}$ inherits the bases of its predecessor $m_{y;n-1}$ because the diffusion term includes the factor $\cos \hat{\mathbf{U}}_y$ as $v_y = v \sin \hat{\mathbf{r}} \cos \hat{\mathbf{U}}_y$.

Provided isotropic scattering is assumed, the collision term generates the isotropic (axially symmetric or azimuthally uniform) component $w_{n;0}$. Here, $w_{n;0} = 0$ for odd n because $m_{y;n}$ for odd n is an odd function with respect to v_y . The amounts of the positive and negative transverse moments completely cancel each other when isotropically scattered electrons are merged in a cell.

Based on the above consideration, we obtain the schematic in Figure 3.

For a summary, some first $m_{y;n}(v; t)$ are expanded as follows:

$$\begin{aligned}
 m_{y,0}(v; \hat{r}; \hat{u}; t) &= w_{0,0}(v; \hat{r}; t) \\
 m_{y,1}(v; \hat{r}; \hat{u}; t) &= w_{1,1}(v; \hat{r}; t) \cos \hat{u} \\
 m_{y,2}(v; \hat{r}; \hat{u}; t) &= w_{2,0}(v; \hat{r}; t) + w_{2,2}(v; \hat{r}; t) \cos^2 \hat{u} \\
 m_{y,3}(v; \hat{r}; \hat{u}; t) &= w_{3,1}(v; \hat{r}; t) \cos \hat{u} + w_{3,3}(v; \hat{r}; t) \cos^3 \hat{u} \\
 m_{y,4}(v; \hat{r}; \hat{u}; t) &= w_{4,0}(v; \hat{r}; t) + w_{4,2}(v; \hat{r}; t) \cos^2 \hat{u} + w_{4,4}(v; \hat{r}; t) \cos^4 \hat{u} \\
 &\vdots
 \end{aligned} \tag{A3}$$

Appendix B. Derivation of the diffusive velocity from the second-order diffusion equation

We consider the electron distribution function of an electron swarm which evolves from a delta function at a point source. Provided the evolution of the distribution function is subject to the second-order diffusion equation, its analytical solution is given as a Gaussian distribution (Huxley and Crompton 1974):

$$\frac{\partial}{\partial t} p(y; t) = R_i p(y; t) + D_T \frac{\partial^2}{\partial y^2} p(y; t) \tag{B1}$$

$$p(y; t) = \frac{N_e(0) \exp(R_i t)}{\sqrt{4D_T t}} \exp\left(-\frac{y^2}{4D_T t}\right) = \frac{N_e(t)}{\sqrt{2\alpha_y}} \exp\left(-\frac{y^2}{2\alpha_y}\right) \tag{B2}$$

where $N_e(t) = N_e(0) \exp(R_i t)$ is the number of electrons. In the case of transverse electron swarm evolution, the first-order derivative term which is related to the drift velocity is missing.

When the diffusive velocity $\bar{v}_y(y; t)$ is defined as the average of v_y at the position y at time t , $\bar{v}_y(y; t)$ is derived by considering the electron flux $\bar{v}_y(y; t)p(y; t)$ crossing a position y towards $+1$. By equating the variation of the number of electrons in the region of $[y; 1]$ with the sum of the electron increase due to ionization and the electron inflow across y , we obtain

$$\frac{d}{dt} \int_y^1 p(y^0; t) dy^0 = \int_y^1 R_i p(y^0; t) dy^0 + \bar{v}_y(y; t) p(y; t) \tag{B3}$$

The electron flux $\bar{v}_y(y; t)p(y; t)$ can be obtained as

$$\begin{aligned}
 \bar{v}_y(y; t)p(y; t) &= \int_y^1 \frac{\partial}{\partial t} \left[\frac{N_e(t)}{\sqrt{4D_T t}} \exp\left(-\frac{y^{02}}{4D_T t}\right) \right] dy^0 \\
 &\quad - \int_y^1 R_i \left[\frac{N_e(t)}{\sqrt{4D_T t}} \exp\left(-\frac{y^{02}}{4D_T t}\right) \right] dy^0 \tag{B4}
 \end{aligned}$$

$$= \int_y^1 \frac{N_e(t)}{\sqrt{4D_T t}} \exp\left(-\frac{y^{02}}{4D_T t}\right) \left[\frac{y^{02}}{4D_T t^2} - \frac{1}{2t} \right] dy^0 \tag{B5}$$

where the partial differential operation in equation (B4) has yielded three terms, but one of them has been canceled out by the second term in the right-hand side (note $\frac{d}{dt}N_e(t) = R_i N_e(t)$).

Here, if we could assume that R_i is independent of y , then

$$\tilde{v}_y(y; t)p(y; t) = \frac{N_e(t)}{4D_T t} \int_{-\infty}^{\infty} \exp\left[-\frac{y^2}{4D_T t} - \frac{y^2}{4D_T t^2} \frac{1}{2t}\right] dy \quad (\text{B6})$$

$$= \frac{N_e(t)}{4D_T t} \exp\left[-\frac{y^2}{4D_T t} - \frac{y^2}{2t}\right] = p(y; t) \frac{y}{2t} \quad (\text{B7})$$

Therefore, we obtain the linear dependence of $\tilde{v}_y(y; t)$ on y as $\tilde{v}_y(y; t) = y/(2t)$.

From equation (B2), the standard deviation $\tilde{\sigma}_y(t)$ of $p(y; t)$ is given as $\tilde{\sigma}_y(t) = \sqrt{2D_T t}$. Thus, the product of the diffusive velocity $\tilde{v}_y(y; t)$ at $y = \tilde{\sigma}_y$ and the standard deviation $\tilde{\sigma}_y$ itself yields the transverse diffusion coefficient D_T

$$\tilde{v}_y(\tilde{\sigma}_y(t); t)\tilde{\sigma}_y(t) = \frac{\sqrt{2D_T t}}{2t} \sqrt{2D_T t} = D_T \quad (\text{B8})$$

References

- Aschwanden T 1985 Thesis Eidgenössischen Technischen Hochschule (ETH), Zürich
- Blevin H A, Fletcher J and Hunter S R 1978 J. Phys. D: Appl. Phys. 11 2295{303}
- Bordage M C, Segur P and Chouki A 1996 J. Appl. Phys. 80 1325{36}
- Braglia G L 1977 Physica 92C 91{112}
- Braglia G L and Baiocchi A 1978 Physica 95C 227{43}
- Date H, Kondo K and Tagashira H 1993 J. Phys. D: Appl. Phys. 26 1211{4}
- Dutton J 1975 J. Phys. Chem. Ref. Data 4 577{858}
- Fletcher J and Reid I D 1980 J. Phys. D: Appl. Phys. 13 2275{83}
- Huxley L E H and Crompton R W 1974 The Diffusion and Drift of Electrons in Gases (New York: Wiley)
- Ikuta N and Murakami Y 1987 J. Phys. Soc. Japan 56 115{27}
- Ikuta N, Takeda A and Yamamoto K 1988 J. Phys. Soc. Japan 57 2401{15}
- Ikuta N and Nakajima S 1993 Trans. IEE Japan 113-A 83{90}
- Itoh H, Miura M, Ikuta N, Nakao Y and Tagashira H 1988 J. Phys. D: Appl. Phys. 21 922{30}
- Itoh H, Matsumura T, Satoh K, Date H, Nakao Y and Tagashira H 1993 J. Phys. D: Appl. Phys. 26 1975{9}
- Kitamori K, Tagashira H and Sakai Y 1980 J. Phys. D: Appl. Phys. 13 535{50}
- Kondo K and Tagashira H 1990 J. Phys. D: Appl. Phys. 23 1175{83}
- Koura K 1986 J. Phys. Soc. Japan 55 2500{3}
- | | 1987 Aust. J. Phys. 40 61{4}
- Kumar K, Skullerud H R and Robson R E 1980 Aust. J. Phys. 33 343{448}
- Kumar K 1981 J. Phys. D: Appl. Phys. 14 2199{208}
- Lowke J J, Phelps A V and Irwin B W 1973 J. Appl. Phys. 44 4664{71}
- Makabe T and Mori T 1984 J. Phys. D: Appl. Phys. 17 699{708}
- Makabe T and Shimoyama M 1986 J. Phys. D: Appl. Phys. 19 2301{8}
- McMahon D R A, Ness K and Shizgal B 1986 J. Phys. B: At. Mol. Phys. 19 2759{77}
- Morrow R 1986 IEEE Trans. Plasma Sci. PS-14 234{9}
- Naidu M S and Prasad A N 1972 J. Phys. D: Appl. Phys. 5 1090{5}
- Penetrante B M, Bardsley J N and Pitchford L C 1985 J. Phys. D: Appl. Phys. 18 1087{100}
- Phelps A V and Pitchford L C 1985 Phys. Rev. A 31 2932{49}
- Pitchford L C, O'Neil S V and Rumble J R Jr 1981 Phys. Rev. A 23 294{304}
- Pitchford L C and Phelps A V 1982 Phys. Rev. A 25 540{54}
- Reid I D 1979 Aust. J. Phys. 32 231{54}
- Robson R E 1995 Aust. J. Phys. 48 677{89}
- Segur P, Yousfi M and Bordage M C 1984 J. Phys. D: Appl. Phys. 17 2199{214}
- Skullerud H R 1974 Aust. J. Phys. 27 195{209}
- Skullerud H R and Kuhn S 1983 J. Phys. D: Appl. Phys. 16 1225{34}
- Skullerud H R 1984 J. Phys. B: At. Mol. Phys. 17 913{29}
- Standish R K 1987 Aust. J. Phys. 40 519{25}
- Sugawara H, Tagashira H and Sakai Y 1997 J. Phys. D: Appl. Phys. 30 368{73}
- Sugawara H, Sakai Y, Tagashira H and Kitamori K 1998 J. Phys. D: Appl. Phys. 31 319{27}
- Tagashira H, Sakai Y and Sakamoto S 1977 J. Phys. D: Appl. Phys. 10 1051{63}
- Tagashira H, Taniguchi T, Kitamori K and Sakai Y 1978 J. Phys. D: Appl. Phys. 11 L43{7}

Viehland L A 1994 Chem. Phys. 179 71{92

Yachi S, Date H, Kitamori K and Tagashira H 1991 J. Phys. D: Appl. Phys. 24 573{80

Yousâ M and Benabdessadok M D 1996 J. Appl. Phys. 80 6619{30

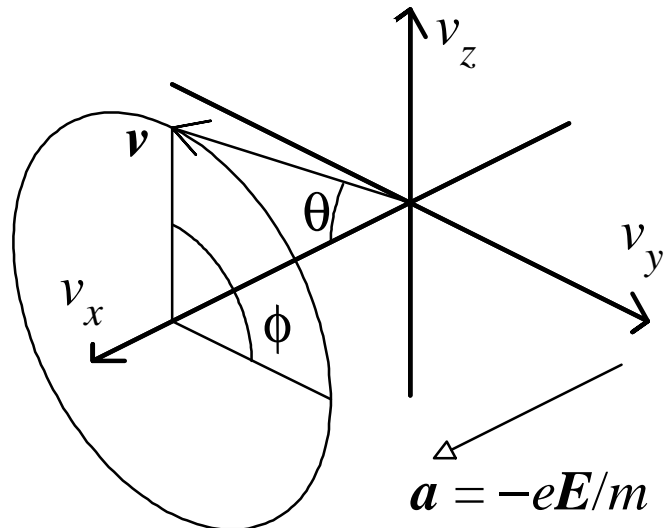


Figure 1. Coordinate variables defined in velocity space. $(v_x; v_y; v_z) = (v \cos \hat{r}; v \sin \hat{r} \cos \hat{c}; v \sin \hat{r} \sin \hat{c})$.

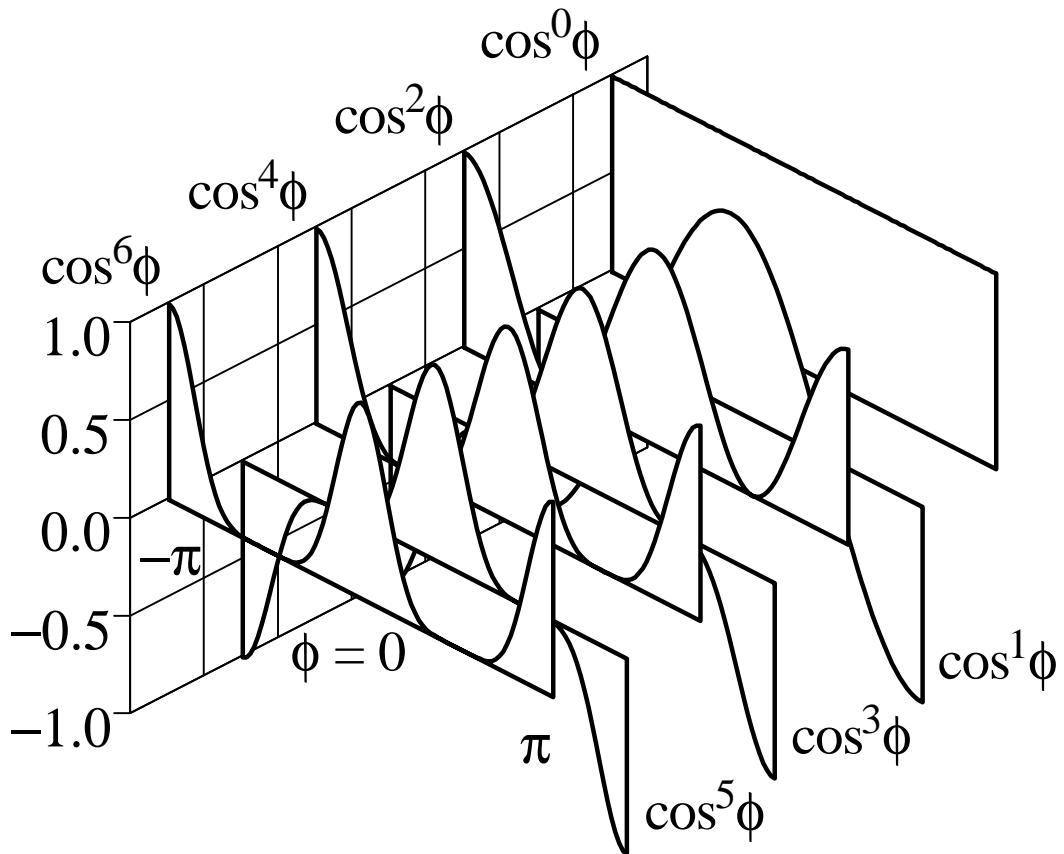


Figure 2. Bases $f \cos^k \hat{c}$ for azimuthal expansion of the transverse moment distribution $m_{y,n}(v; \hat{r}; \hat{c}; t)$. The distribution is localized around $\hat{c} = 0$ and $\hat{c} = \hat{U} \hat{c}$. Note that $f \cos^k \hat{c}$ is not an orthogonal system of functions.

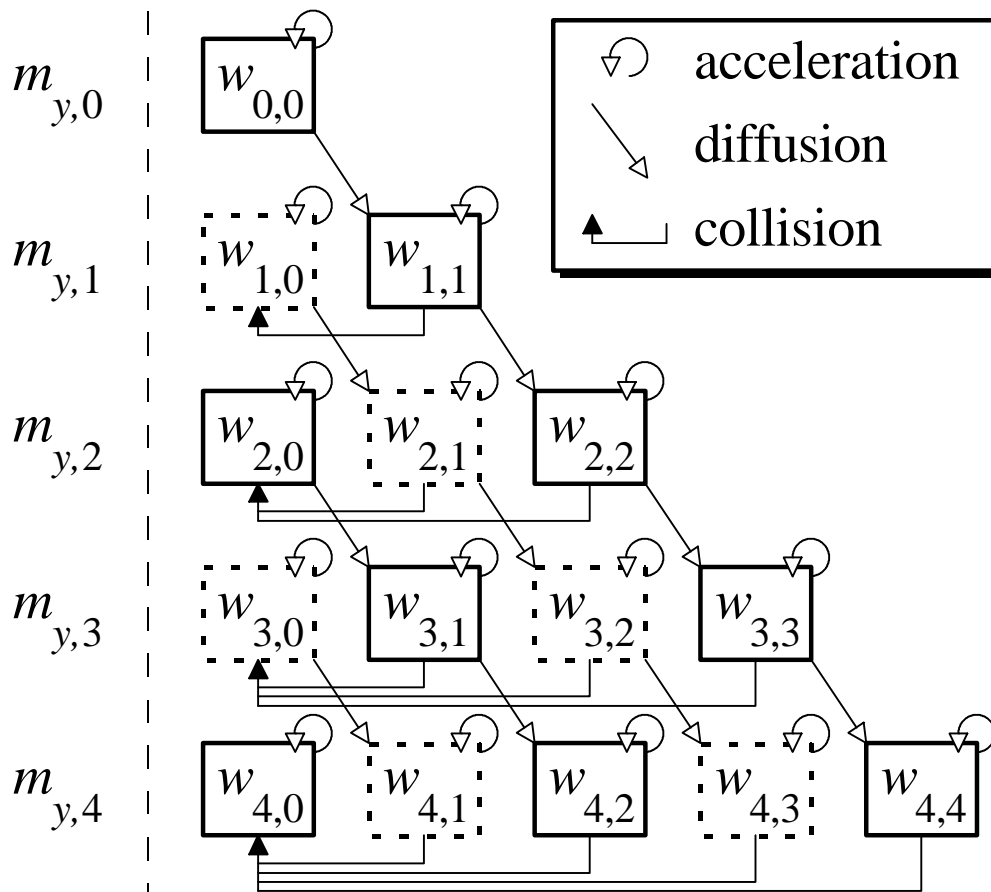


Figure 3. Schematic for inter-component action of the azimuthal components $w_{n,k}(v; \hat{r}; t)$ due to the acceleration, diffusion and collision terms in the moment equations. Dashed squares indicate that $w_{n,k}$ for $n \not\equiv k \pmod{2}$ within are always zero.

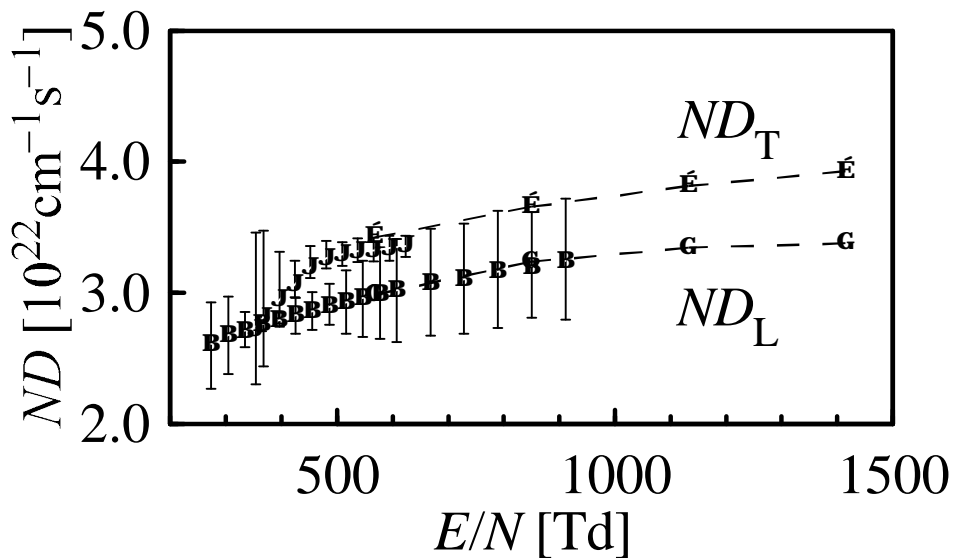


Figure 4. A comparison between the results of experimental measurements and the present calculation; full circles, Naidu and Prasad (1972); full squares, Aschwanden (1985); open circles and open squares, present calculation.

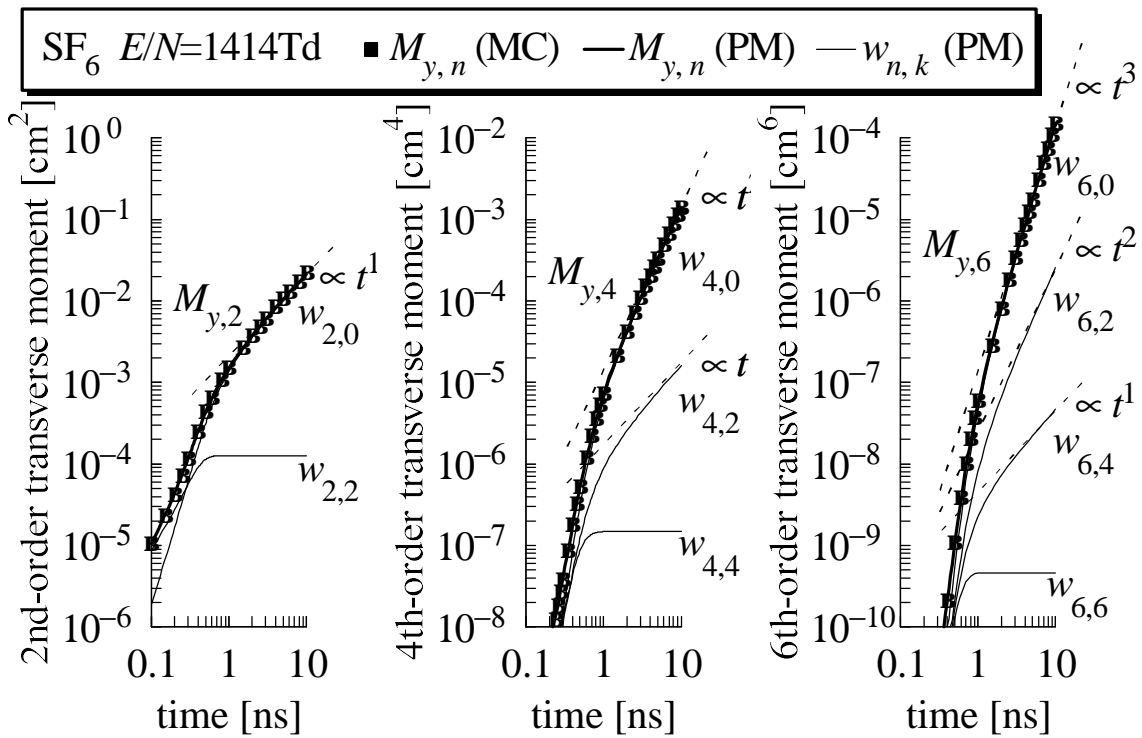


Figure 5. Evolution of the azimuthal components of the transverse moments in SF_6 at $E/N = 1414 \text{ Td}$. $M_{y;n}$ and $w_{n;k}$ have been integrated throughout velocity space. Here the curves of $w_{n,0}$ are nearly hidden by those of $M_{y;n}$. It is indicated that $w_{n,k} \propto t^{(n-k)/2}$ after relaxation.

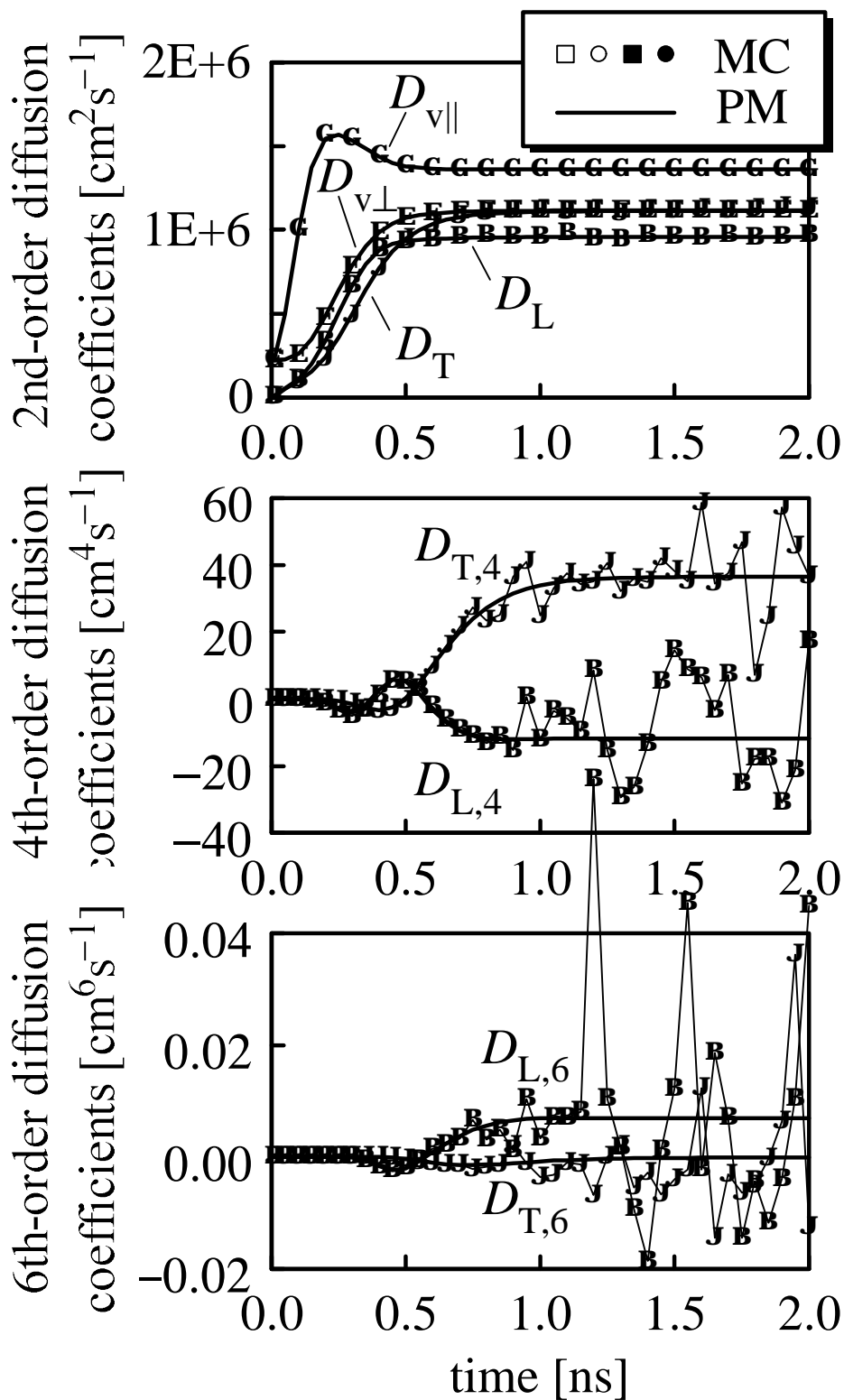


Figure 6. Relaxation of the electron diffusion coefficients in SF₆ at E/N = 1414 Td: squares and circles, Monte Carlo simulation; and full curves, propagator method. $D_{T;n}$ and $D_{L;n}$ are derived from the transverse and longitudinal electron distributions in real space. $D_{v\perp}$ and $D_{v\parallel}$ are derived from the velocity distributions in the perpendicular and parallel direction to the applied electric field.

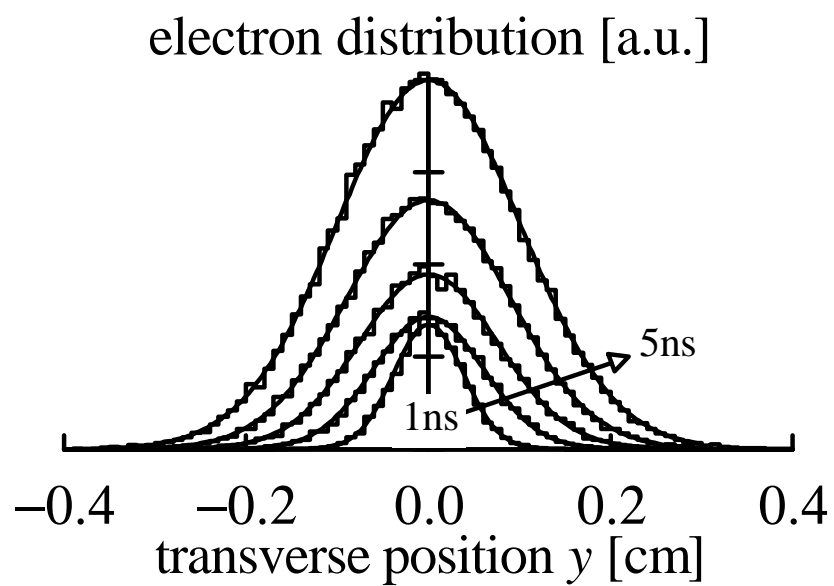


Figure 7. The transverse electron distribution function $p(y; t)$ in SF_6 at $E=N = 1414 \text{ Td}$ ($t = 1, 2, 3, 4$ and 5 ns): histogram, Monte Carlo simulation; and full curve, propagator method.

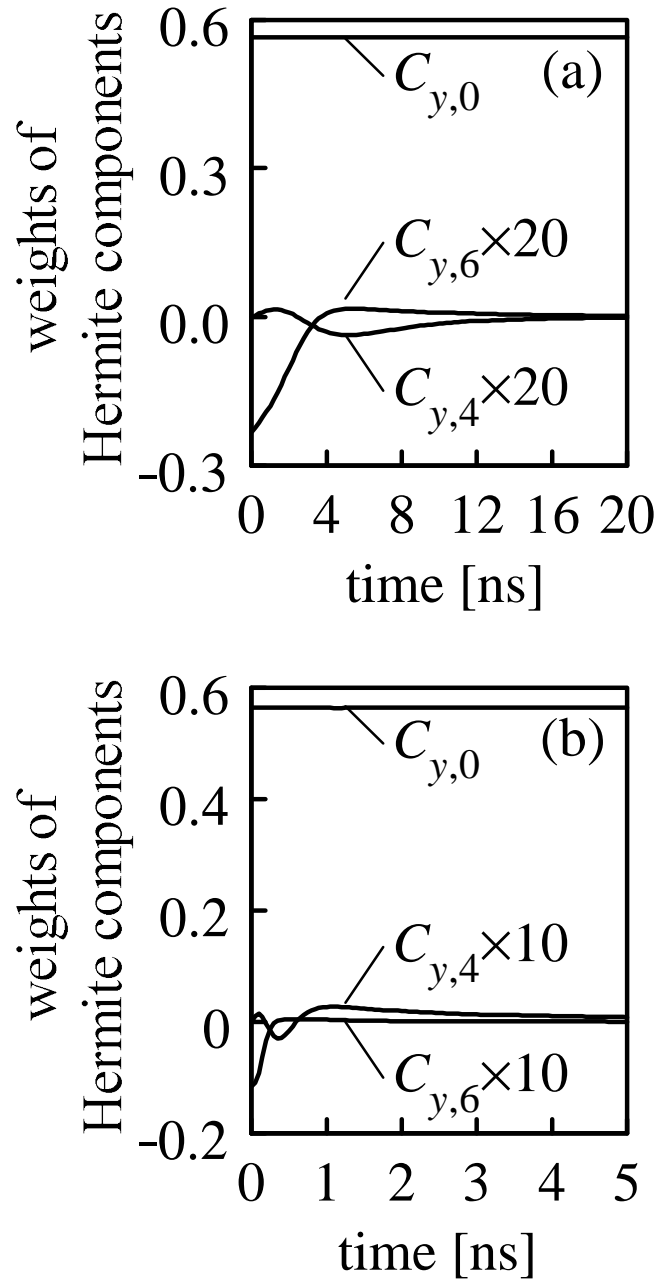


Figure 8. The weights of Hermite components of the transverse electron distribution in (a) ramp model gas (Reid 1979) at $E=N = 24$ Td and (b) SF_6 at $E=N = 1414$ Td. Higher-order $C_{y,n}$ represent the deviation of a distribution shape from a Gaussian distribution.

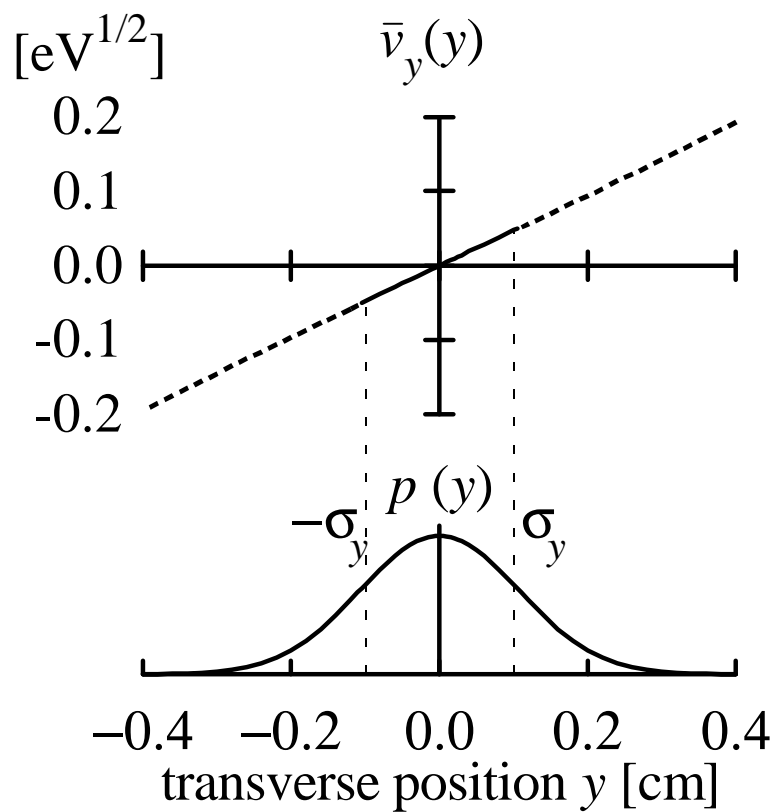


Figure 9. Gaussian shape of the transverse electron distribution and linear dependence of the transverse drift velocity on the transverse position: ramp model gas (Reid 1979) at $E/N = 24$ Td at 20 ns after the release of the initial electrons.

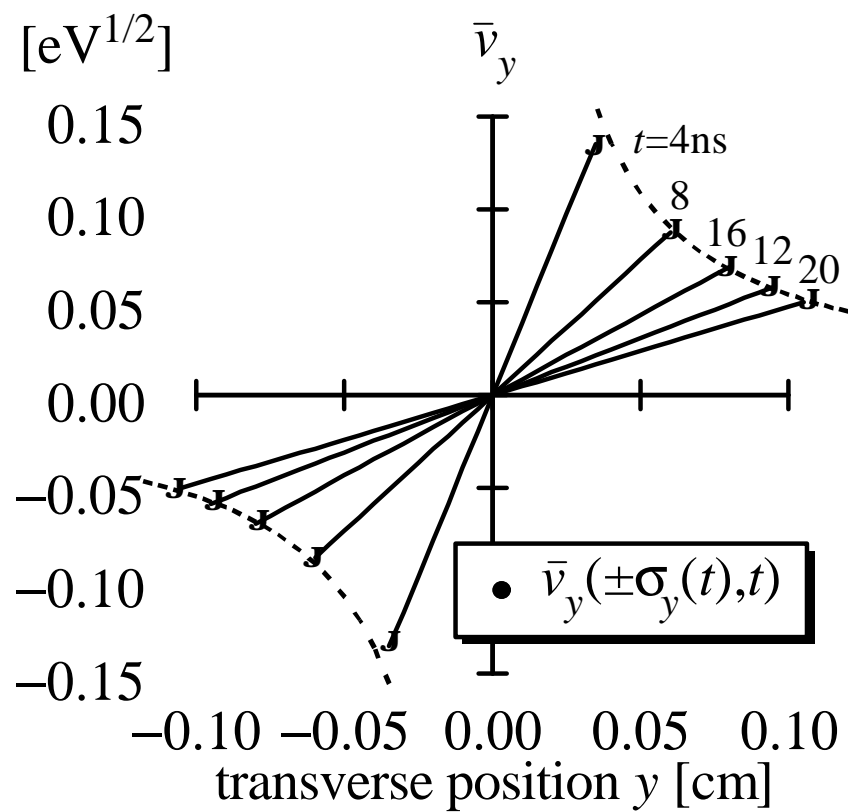


Figure 10. Temporal variation of the linear dependence of the transverse dispersive velocity $\bar{v}_y(y;t)$ in the range $-\bar{\sigma}_y \leq y \leq \bar{\sigma}_y$ in ramp model gas. $\bar{v}_y(\bar{\sigma}_y)$ is inversely proportional to $\bar{\sigma}_y$.

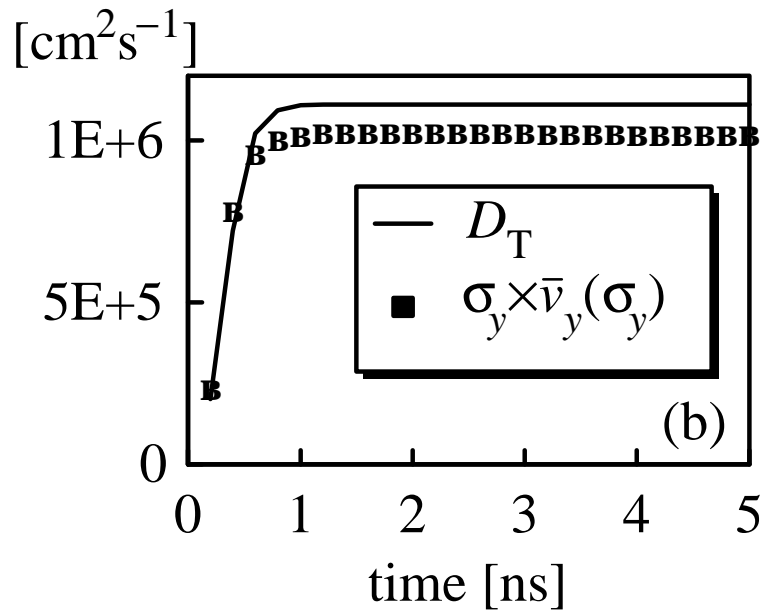
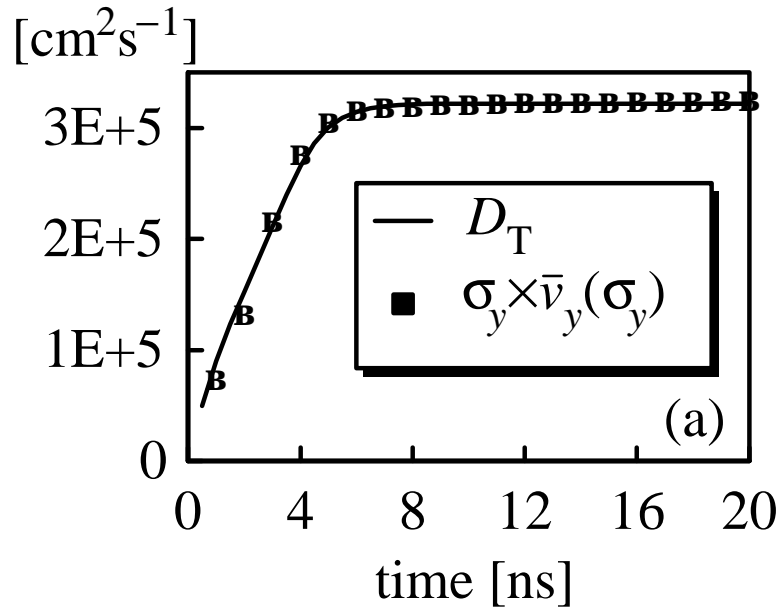


Figure 11. The transverse diffusion coefficient D_T and the product of the standard deviation $\bar{\sigma}_y$ and the diffusive velocity \bar{v}_y at the position $y = \bar{\sigma}_y$: (a) ramp model gas (Reid 1979) at $E=N = 24 \text{ Td}$ (the number of electrons is conservative) and (b) SF_6 at $E=N = 1414 \text{ Td}$ (ionization-dominated case).

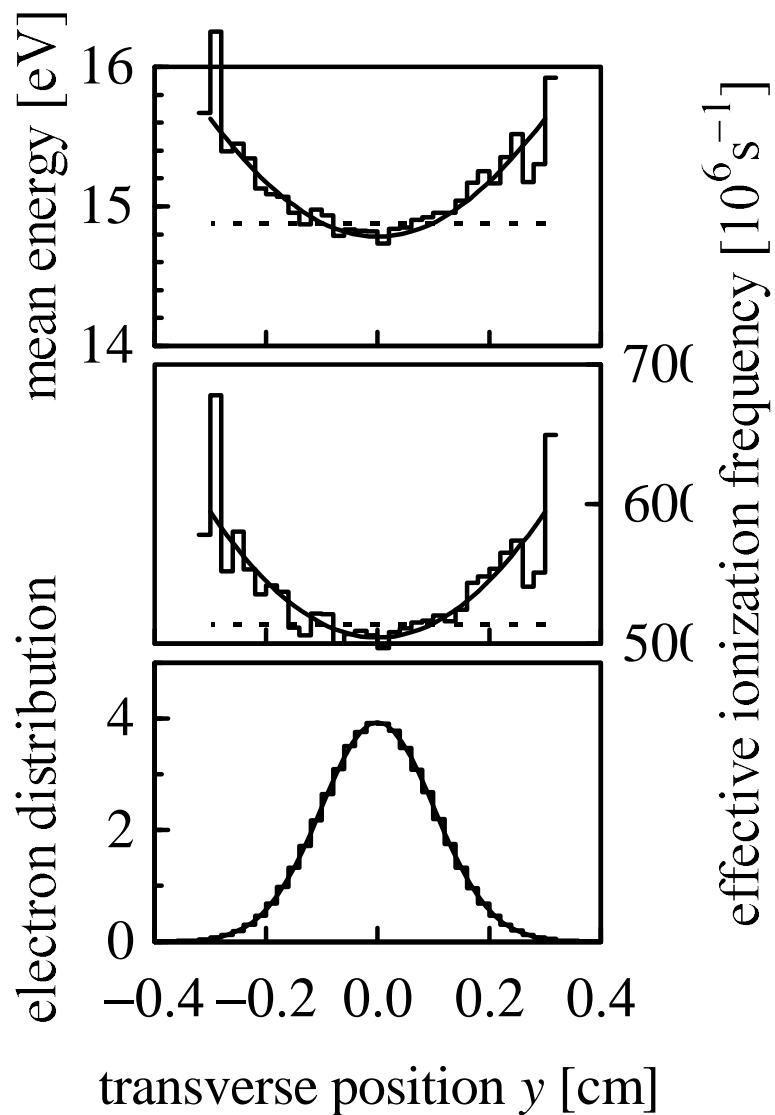


Figure 12. The transverse electron distribution and local values of the mean electron energy and the effective ionization frequency at the position y in SF_6 at $E=N = 1414 \text{ Td}$ at $t = 5 \text{ ns}$: histogram, Monte Carlo simulation; and full curve, propagator method. The broken lines indicate their global averages calculated by the propagator method.